Journal of Solid State Chemistry **154,** 591–597 (2000)
doi:10.1006/jssc.2000.8900, available online at http://www.idealibrary.com on IDEAL®

Magnetic Susceptibilities and Mössbauer Spectra of Perovskites A_2FeNbO_6 (A = Sr, Ba)

Keitaro Tezuka, Kou Henmi, and Yukio Hinatsu

Division of Chemistry, Graduate School of Science, Hokkaido University, Sapporo 060-0810, Japan

and

Nobuyuki M. Masaki

Japan Atomic Energy Research Institute, Tokai-mura, Ibaraki 319-1195, Japan

Received May 1, 2000; accepted July 28, 2000; published online September 30, 2000

Perovskite-type compounds A_2FeNbO_6 (A = Sr, Ba) were prepared. Their powder X-ray diffraction measurements and the Rietveld analysis show that the cations Fe^{3+} and Nb^{5+} over the six-coordinate sites of the perovskite structure are arranged randomly for Sr_2FeNbO_6 and some of them order regularly for Ba_2FeNbO_6. They show magnetic susceptibility maxima at ca. 25 K. Below the temperatures, the divergence of the magnetic susceptibilities measured between the zero-field-cooled condition and the field-cooled condition has been measured. Field-cooled and zero-field-cooled susceptibilities show a hysteresis below maximum temperatures. These results indicate the existence of a ferromagnetic component in the magnetic moment. Mössbauer spectra measured at 6 K comprise a single magnetic hyperfine pattern typical of Fe^{3+}, but with a high degree of line broadening. These data are discussed in terms of antiferromagnetic interactions with a ferromagnetic component. © 2000 Academic Press

INTRODUCTION

The perovskite-type oxides have the general formula ABO_3, in which A represents a large electropositive cation and B represents a small transition metal ion. The perovskite structure can be described as a framework of corner-shared BO_6 octahedra which contain A cations at 12-coordinate sites. Double perovskite-type oxides have the formula $A_2B'B''O_6$, in which the primes indicate the different ions in different oxidation states, and in some cases, the cations at the B sites, B' and B'', regularly order, i.e., 1:1 arrangement of B' and B'' ions has been observed over the six-coordinate B sites. Since the B cations generally determine the physical properties of perovskites, different kinds of B' and B'' ions should show a variety of the physical properties of double perovskites. Battle *et al.* reported crystal chemistry and magnetic properties of many double perovskites containing transition elements (1–3).

We have paid attention to the structural chemistry and magnetic properties of ordered perovskite-type oxides A_2LnMO_6 (A = Sr, Ba; Ln = lanthanide elements; M = 4d or 5d transition elements) in which the Ln and M ions order shows a range of magnetic behavior at low temperatures (4), (5). Recently, it has become clear that the magnetic properties of some mixed-metal oxides are often more complex than were previously recognized. Rodríguez *et al.* reported that the cubic perovskite Sr_2FeNbO_6 shows a spin glass transition from the magnetic susceptibility and hysteresis loop measurements (6). This compound is an insulator with a disordered distribution of magnetic Fe^{3+} and nonmagnetic Nb^{5+} ions within a unique octahedral site, hence forming a diluted simple cubic lattice. They suggested that short-range structural ordering of Fe^{3+} and Nb^{5+} was responsible for the observed magnetic behavior and pointed out that this was the first time that a spin glass transition was identified in an insulator having a nonfrustrated lattice and only antiferromagnetic interactions. However, subsequent EXAFS and Mössbauer studies failed to find any evidence for such an ordering (7). Battle *et al.* investigated the series of A_2FeMO_6 (A = Ca, Sr, Ba; M = Nb, Ta, Sb) by X-ray powder diffraction, magnetic susceptibility, and Mössbauer spectroscopy and discussed the data obtained for some compounds in terms of spin-glass behavior (3).

In this study, we focus our attention on the crystal structure and magnetic properties of both the compounds Sr_2FeNbO_6 and Ba_2FeNbO_6. Although the former compound was discussed to show spin glass behavior at low temperatures from magnetic susceptibility and hysteresis loop measurements, experimental results of Mössbauer spectrum and EXAFS measurements did not support it. In addition, Rodríguez *et al.* reported that the crystal

0022-4596/00 $35.00

symmetry of Sr_2FeNbO_6 was cubic (6), but it was discussed to be orthorhombic by the following research. To elucidate these experimental inconsistencies, we have carried out X-ray powder diffraction experiments for both the compounds and analyzed their crystal structures by the Rietveld method. The magnetic properties were elucidated by the measurements of the magnetic susceptibility and thermal remnant magnetization (in the temperature range between 4.5 and 300 K, under both zero-field-cooled and field-cooled conditions), magnetic hysteresis (at 4.5 K, under both zero-field-cooled and field-cooled conditions), and Mössbauer spectra (at 6 K and room temperature).

EXPERIMENTAL

1. Sample Preparation

Polycrystalline samples of A_2FeNbO_6 (A = Sr, Ba) were prepared by the conventional ceramic method using starting materials $SrCO_3$ ($BaCO_3$), Fe_2O_3, and Nb_2O_5. These starting materials were weighed in the correct ratios, mixed well in an agate mortar, and then pressed into pellets. The pellets were heated in air at 1200°C for 60 h with several interval grindings, and finally at a temperatures up to 1300°C for 12 h. Then, they were slowly cooled to room temperature in the furnace to obtain the oxygen stoichiometric compounds.

2. X-ray Diffraction Analysis

X-ray diffraction profiles of the powdered samples were obtained with Rigaku RINT 2000 diffractometer using monochromatized Cu$K\alpha$ radiation. For their Rietveld analysis, intensity data were collected at each 0.02° step for 5 s over a 2θ range of 10–110°.

3. Magnetic Susceptibility Measurements

Magnetic susceptibility measurements were made using a SQUID magnetometer (Quantum Design MPMS). Data

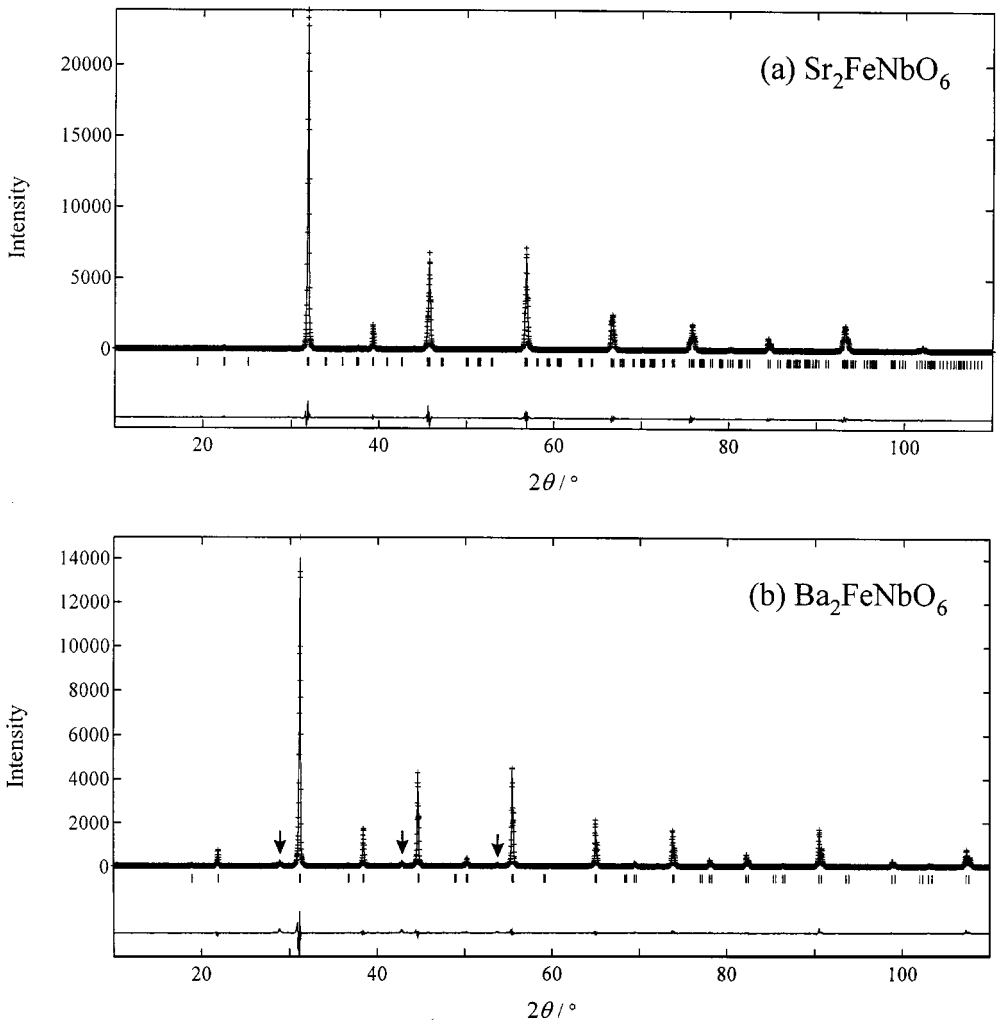

FIG. 1. X-ray diffraction profiles for Sr_2FeNbO_6 (a) and Ba_2FeNbO_6 (b). The calculated and observed patterns are shown on the top solid line and cross markers, respectively. The vertical marks in the middle show positions calculated for Bragg reflections. The trace on the bottom is a plot of the difference between calculated and observed intensities. Arrows in the diffraction profile of Ba_2FeNbO_6 correspond to diffraction peaks for an impurity $Ba_5Nb_4O_{15}$.

were collected after cooling the sample in the absence of an applied magnetic field (zero-field-cooled (ZFC)) and after cooling in the magnetic field (field-cooled (FC)) of 0.1 T. In addition to these measurements, measurements for monitoring the field dependence of the magnetic susceptibility and the existence of a thermal remnant magnetization were also carried out.

4. Mössbauer Spectrum Measurements

The Mössbauer spectra were measured with a conventional transmissional Mössbauer spectrometer operating in the constant acceleration mode. Absorbers were prepared of finely ground Sr_2FeNbO_6 and Ba_2FeNbO_6, in each case weighed to give optimum signal-to-noise and mixed with carbon to randomize the orientations of the microcrystals. A source of up to 100 mCi of ^{57}Co in Rh was used and the spectrometers were calibrated using α-iron at room temperature. The spectra at 6 K were measured with an Oxford flow cryostat.

TABLE 1
Crystal Structure Data for Sr_2FeNbO_6 and Ba_2FeNbO_6 from X-ray Diffraction Profiles

Atom	Position	x	y	z	g	B (Å^2)
Sr_2FeNbO_6 space group *Pnma* (No. 62) $a = 5.6082(9)$ Å $b = 7.9642(1)$ Å $c = 5.6084(9)$ Å $R_{wp} = 12.68\%$ $R_I = 2.93\%$ $R_F = 4.91\%$ $R_e = 7.91\%$						
Sr	4*c*	− 0.002(3)	$\frac{1}{4}$	− 0.003(2)	1	0.75
Fe, Nb	4*b*	0	0	$\frac{1}{2}$	1	0.43
O(1)	4*c*	0.506(16)	$\frac{1}{4}$	0.048(5)	1	0.61
O(2)	8*d*	0.259(65)	0.508(5)	0.243(79)	1	0.73
Ba_2FeNbO_6 space group $Fm\bar{3}m$ (No. 225) $a = 8.1181(1)$ Å $R_{wp} = 16.68\%$ $R_I = 2.49\%$ $R_F = 4.02\%$ $R_e = 10.05\%$						
Ba	8*c*	$\frac{1}{4}$	$\frac{1}{4}$	$\frac{1}{4}$	1	0.64
Fe1	4*a*	0	0	0	0.68(9)	0.39
Fe2	4*b*	$\frac{1}{2}$	$\frac{1}{2}$	0	0.32(9)	0.36
Nb1	4*a*	0	0	0	0.32(9)	0.34
Nb2	4*b*	$\frac{1}{2}$	$\frac{1}{2}$	$\frac{1}{2}$	0.68(9)	0.38
O(2)	24*e*	0.253(9)	0	0	1	0.56

RESULTS AND DISCUSSION

X-ray Diffraction

Perovskites with general composition $A_2M_1^{3+}M_2^{5+}O_6$ have a tendency to the atomic ordering of M_1 and M_2 ions, and in some cases, the perovskite lattice parameters become double, indicating the setting of a long-range crystallographic ordering of metallic ions. The X-ray powder diffraction profiles collected for Sr_2FeNbO_6 and Ba_2FeNbO_6 are shown in Figs 1a and 1b, respectively. The profile for Sr_2FeNbO_6 shows no existence of the superlattice reflection at $2\theta \sim 19^\circ$ and it could be indexed in the orthorhombic space group *Pnma*. This space group does not permit the ordering of the cations Fe^{3+} and Nb^{5+} over the six-coordinate sites of the perovskite structure. In the profile for Ba_2FeNbO_6, there is a very small superlattice reflection at $2\theta \sim 19^\circ$ and it could be indexed in the cubic space group $Fm\bar{3}m$, i.e., the cations Fe^{3+} and Nb^{5+} order regularly. The results of our Rietveld analysis indicate that about one-third of the *B* site cations order (8, 9). The Rietveld fittings are shown in Fig. 1 and the crystal structural parameters are listed in Table 1.

Magnetic Susceptibility

Figures 2 and 3 show the temperature dependence of the ZFC and FC magnetic susceptibilities for Sr_2FeNbO_6 and Ba_2FeNbO_6, respectively. Both the compounds show similar magnetic behavior, i.e., the ZFC susceptibilities have maxima at ca. 25 K (T_{max}), and the divergence of the ZFC and FC susceptibilities has been found below this temperature. Hysteresis is apparent in the susceptibilities below T_{max}, but not at higher temperatures. Figures 4 and 5 show the magnetic hysteresis loops measured at $T = 4.5$ K after ZFC (magnetic field sweeping ± 5 T) and after cooling from room temperature under $H = 5$ T (FC) for Sr_2FeNbO_6 and Ba_2FeNbO_6, respectively. Small magnetic hysteresis has been observed for both ZFC and FC susceptibilities and

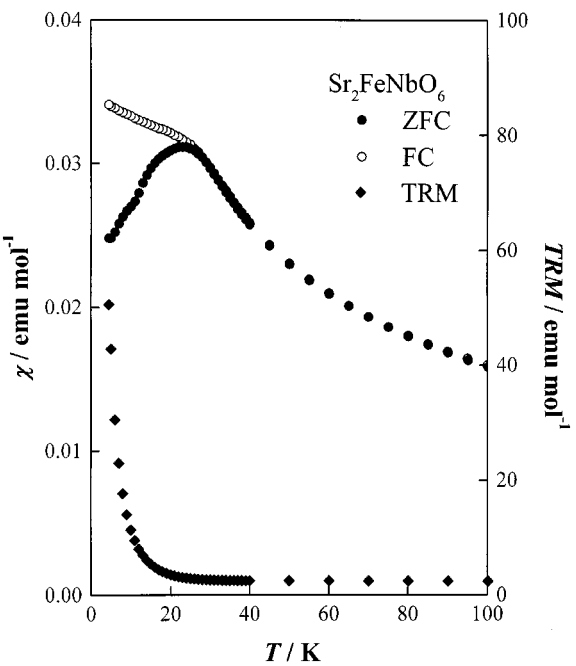

FIG. 2. Temperature dependence of the ZFC and FC magnetic susceptibilities for Sr_2FeNbO_6. The temperature dependence of the thermal remnant magnetization (TRM) is also shown.

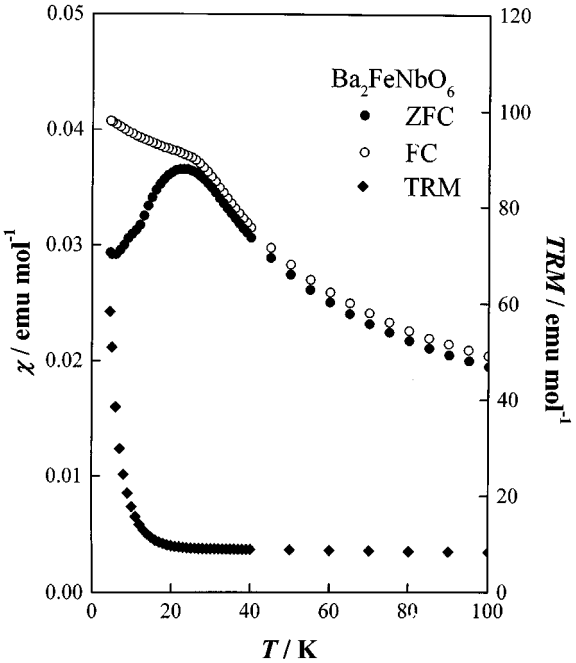

FIG. 3. Temperature dependence of the ZFC and FC magnetic susceptibilities for Ba_2FeNbO_6. The temperature dependence of the thermal remnant magnetization (TRM) is also shown.

their hysteresis loops are quite similar to each other. The results of the thermal remnant magnetization measurements for Sr_2FeNbO_6 and Ba_2FeNbO_6 are also shown in Figs. 2 and 3, respectively. The thermal remnant magnetization falls rapidly as the temperature is increased, becoming immeasurably small at T_{max}. These experimental results indicate that the magnetic moments of Fe^{3+} ions in Sr_2FeNbO_6 and Ba_2FeNbO_6 order antiferromagnetically with a slight ferromagnetic moment below ca. 25 K, and the weak ferromagnetic moments disappear above ca. 25 K; i.e., it has been confirmed that the magnetic moments of Fe^{3+} ions showing antiferromagnetic interactions at low temperatures have a weak ferromagnetic component below the Néel temperatures. Our conclusion on the magnetic properties of Sr_2FeNbO_6 contradicts the discussion by Rodríguez *et al.* that Sr_2FeNbO_6 shows no magnetic phase transition above 32.5 K but behaves as a spin glass below that temperature and that short-range structural ordering of Fe^{3+} and Nb^{5+} is responsible for the observed behavior (6). Their discussion is based on the observation of the hysteresis loops in which a uniaxial anisotropy is induced in the field cooling process. However, subsequent EXAFS and Mössbauer studies failed to find any evidence for such a short-range structural ordering (7). Our experimental results on the hysteresis measurements are that hysteresis loops measured after zero field cooling and those measured after field cooling are quite similar to each other.

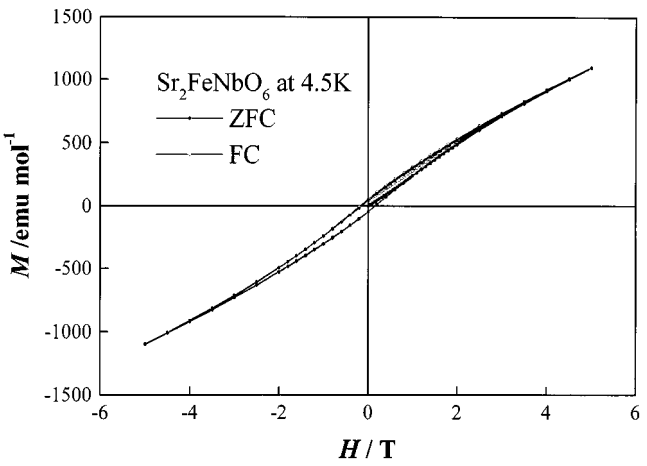

FIG. 4. Magnetic hysteresis loops of Sr_2FeNbO_6 measured at $T = 4.5$ K after zero field cooling (ZFC) and after cooling from room temperature under $H = 5$ T (FC).

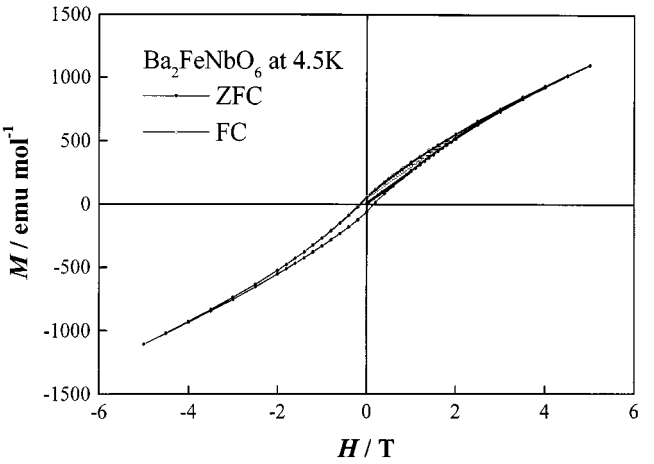

FIG. 5. Magnetic hysteresis loops of Ba_2FeNbO_6 measured at $T = 4.5$ K after zero field cooling (ZFC) and after cooling from room temperature under $H = 5$ T (FC).

Figure 6 shows the reciprocal ZFC magnetic susceptibility as a function of temperature for Sr_2FeNbO_6 and Ba_2FeNbO_6. A linear relationship has been found above 200 K for the Sr_2FeNbO_6; i.e., a Curie–Weiss law holds with a Curie constant $C = 3.90\ \mathrm{K\,mol^{-1}}$ and a Weiss temperature $\Theta = -173$ K. For Ba_2FeNbO_6, no linearity has been found for the reciprocal susceptibility vs temperature curve in the experimental temperature range.

The large value of the Weiss constant indicates that strong antiferromagnetic interactions operate among the Fe^{3+} ions. The effective magnetic moments of the Fe^{3+} ions in the Sr_2FeNbO_6 are determined to be 5.59 μ_B. This value is a little lower than the effective magnetic moments for the Fe^{3+} ion in a high-spin configuration, 5.92 μ_B. The reason for this is that some antiferromagnetic interactions among the spins have developed.

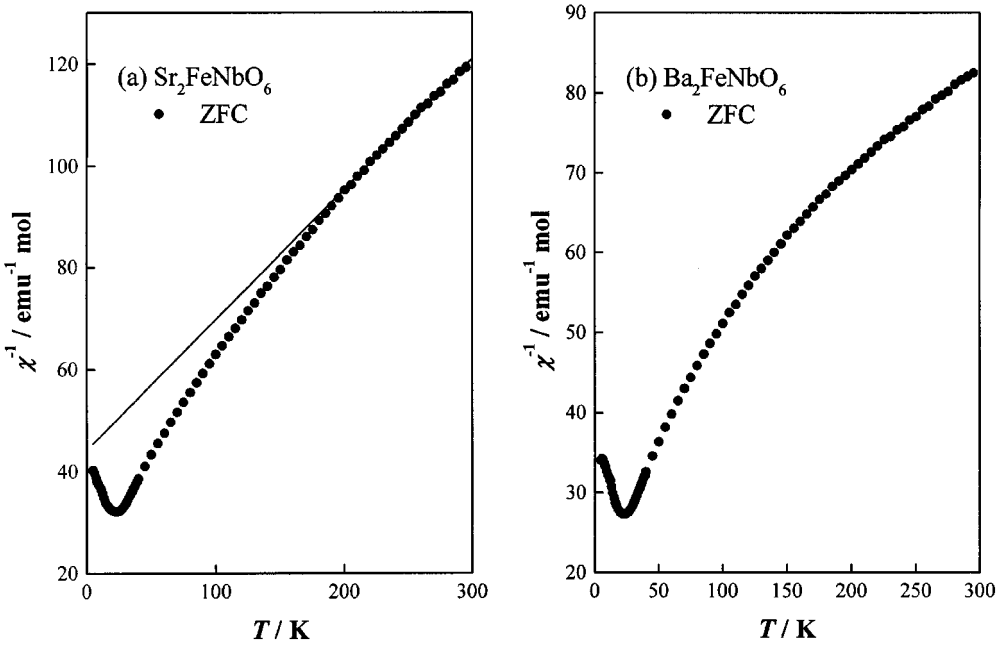

FIG. 6. The reciprocal magnetic susceptibilities as a function of temperature for Sr_2FeNbO_6 (a) and Ba_2FeNbO_6 (b).

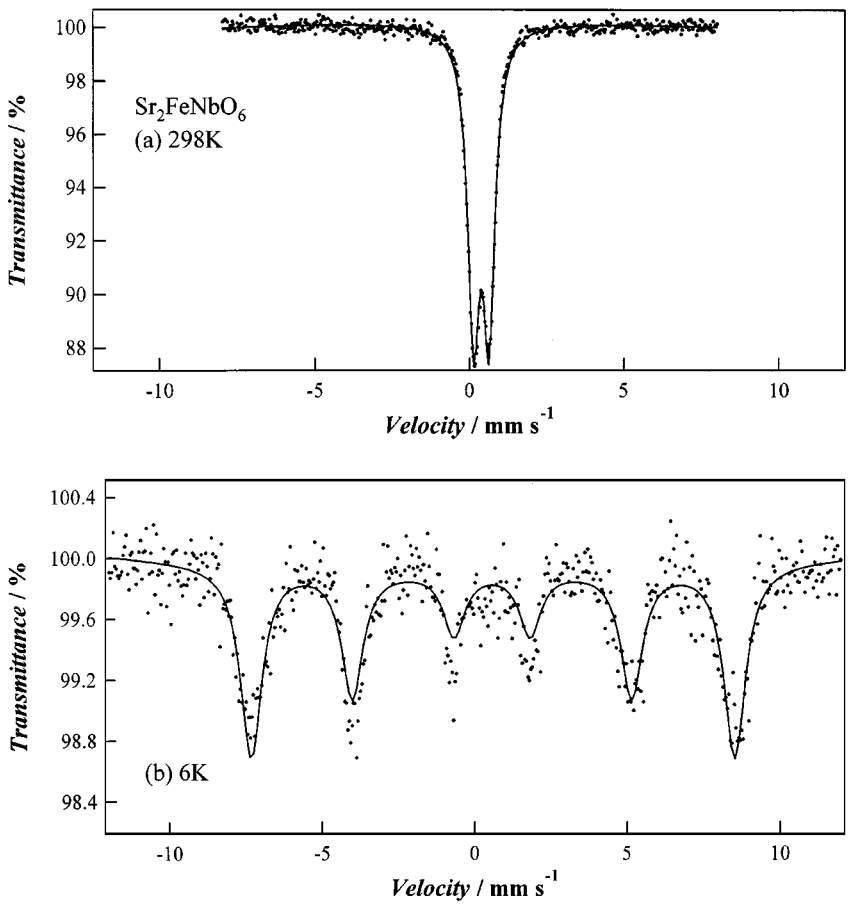

FIG. 7. Mössbauer spectra of Sr_2FeNbO_6 measured at 298 K (a) and at 6 K (b). The calculated spectra are shown by the solid lines, and the determined Mössbauer parameters are given in Table 2.

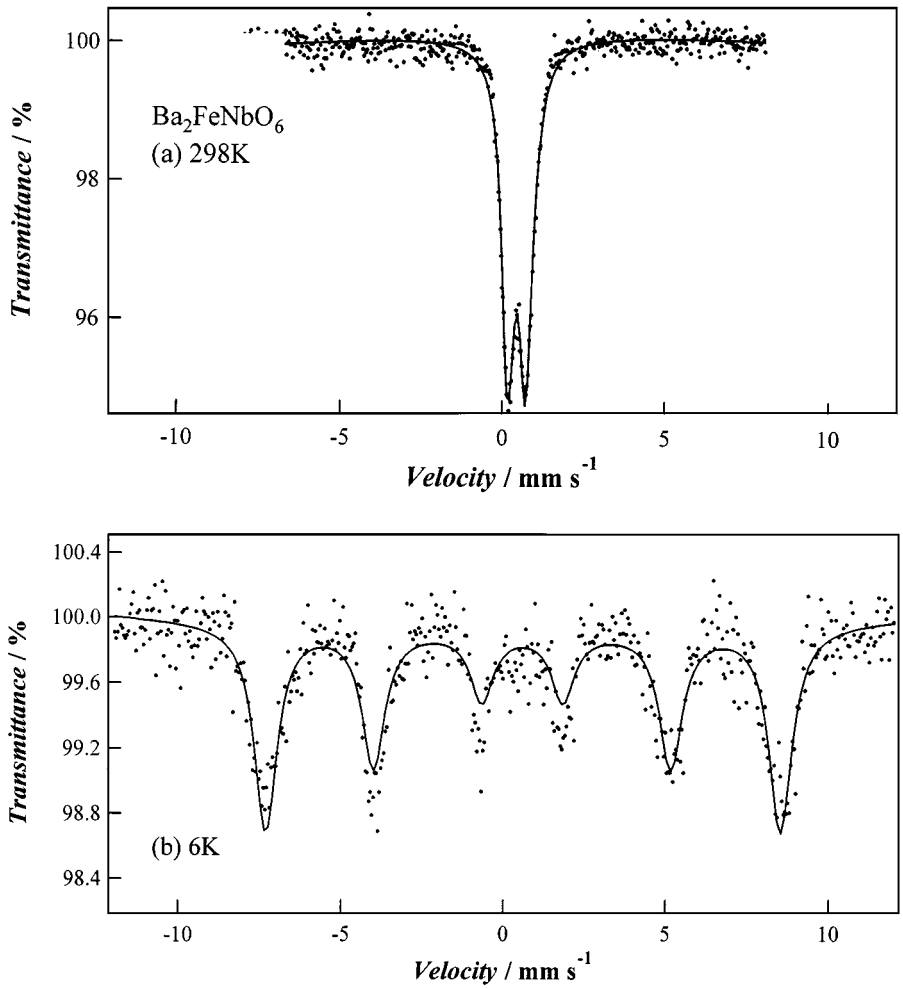

FIG. 8. Mössbauer spectra of Ba_2FeNbO_6 measured at 298 K (a) and at 6 K (b). The calculated spectra are shown by the solid lines, and the determined Mössbauer parameters are given in Table 2.

Mössbauer Spectrum

The Mössbauer spectra of Sr_2FeNbO_6 and Ba_2FeNbO_6 measured at room temperature and at 6 K are shown in Figs 7 and 8, respectively. The spectra of Sr_2FeNbO_6 resemble those of Ba_2FeNbO_6 at both the temperatures. The spectra measured at room temperature show a simple quadrupole doublet, which indicates the existence of the electric field gradient, i.e., the symmetry at the Fe site in a lattice is no longer cubic. The large charge difference between Fe^{3+} and Nb^{5+} together with the local structural distributions in a disordered material produces the large splitting. The present Mössbauer spectra indicate that the cations on the *B* sites disorder in both the Sr_2FeNbO_6 and Ba_2FeNbO_6. Experimental spectra were reproduced by a single-doublet fitting, and the obtained Mössbauer parameters, the isomer shift (δ), the quadrupole splitting (ε), and the linewidth (Γ) are listed in Table 2. The isomer shifts have established that the Fe is in the trivalent oxidation state. The parameter values vary little between the two compounds except for the isomer shift. The isomer shift is more positive for Ba_2FeNbO_6 compared with that of Sr_2FeNbO_6.

The Mössbauer spectra measured at 6 K show a single magnetic hyperfine pattern typical of Fe^{3+}, but with a high degree of line broadening. The Mössbauer parameters were obtained by fitting the spectra, and they are listed in Table 2. The parameter values vary little between Sr_2FeNbO_6 and Ba_2FeNbO_6 except for the isomer shift; i.e., the more positive isomer shift is obtained for Ba_2FeNbO_6, which is consistent with the result at room temperature. Compared with the spectra at room temperature, the linewidths of the spectra at 6 K have broadened. The quadrupole splittings are so small as to be effectively zero for both the compounds. Therefore, we can discuss that the large electric field gradients which are apparent from the paramagnetic spectra at room temperature must have comparatively ran-

TABLE 2
Mössbauer Parameters

Sr_2FeNbO_6			
T (K)	298		6
δ (mm/s)	0.390(1)	δ (mm/s)	0.481(10)
ε (mm/s)	0.250(1)	ε (mm/s)	0.001(9)
Γ (mm/s)	0.462(4)	Γ (mm/s)	0.894(37)
		B_{hf} (T)	48.71(7)
Ba_2FeNbO_6			
T (K)	298		6
δ (mm/s)	0.445(2)	δ (mm/s)	0.588(12)
ε (mm/s)	0.278(2)	ε (mm/s)	0.010(12)
Γ (mm/s)	0.494(7)	Γ (mm/s)	0.843(41)
		B_{hf} (T)	49.30(8)

dom orientations with respect to the spin axis. This may cause the large linewidths observed in the spectra measured at 6 K. The results on the Mössbauer spectrum measurements have been found to be quite similar between Sr_2FeNbO_6 and Ba_2FeNbO_6.

ACKNOWLEDGMENT

This work was supported by a Grant-in-Aid for scientific research on priority area "Novel Quantum Phenomena in Transition Metal Oxides-Spin · Charge · Orbital Coupled Systems" from the Ministry of Education, Science, Sports, and Culture of Japan.

REFERENCES

1. P. D. Battle and C. W. Jones, *J. Solid State Chem.* **78,** 108 (1989).
2. P. D. Battle, T. C. Gibb, C. W. Jones, and F. Studer, *J. Solid State Chem.* **78,** 281 (1989).
3. P. D. Battle, T. C. Gibb, A. J. Herod, S.-H. Kim, and P. H. Munns, *J. Mater. Chem.* **5,** 865 (1995).
4. D. Harada, M. Wakeshima, and Y. Hinatsu, *J. Solid State Chem.* **145,** 256 (1999).
5. Y. Doi and Y. Hinatsu, *J. Phys. Condens. Matter.* **11,** 4813 (1999).
6. R. Rodríguez, A. Fernández, A. Isalgué, J. Rodríguez, A. Labarta, J. Tejada, and X. Obradors, *J. Phys. C: Solid State Phys.* **18,** L401 (1985).
7. T. C. Gibb, *J. Mater. Chem.* **3,** 441 (1993).
8. T. Nakagawa and S. Nomura, *J. Phys. Soc. Jpn.* **21,** 1468 (1966).
9. M. Wakeshima, D. Harada, and Y. Hinatsu, *J. Alloys. Compd.* **287,** 130 (1999).